HOKKAIDO UNIVERSITY

Title	Spectroscopic investigations of photothermal and photochemical activities of electron donor-acceptor molecular dyads [an abstract of entire text]
Author(s)	Sasikumar, Devika
Citation	北海道大学. 博士(環境科学) 甲第13897号
Issue Date	2020-03-25
Doc URL	http://hdl.handle.net/2115/78591
Type	theses (doctoral - abstract of entire text)
Note	この博士論文全文の閲覧方法については、以下のサイトをご参照ください。
Note(URL)	https://www.lib.hokudai.ac.jp/dissertations/copy-guides/
File Information	Sasikumar_Devika_summary.pdf

Instructions for use

Hokkaido University Collection of Scholarly and Academic Papers : HUSCAP

Spectroscopic investigations of photothermal and photochemical activities of electron donor-acceptor molecular dyads

（電子ドナー・アクセプター連結分子による光熱変換および光化学反応についての分光学的研究）

Photoinduced electron transfer (PET) is an extensively investigated and explored phenomenon in the field of chemistry and biology. By considering the contribution of electron transfer systems in natural photosynthesis, diverse artificial molecular systems have been developed and utilized for solar energy harnessing. The applications of electron transfer are not limited to solar harvesters only but also enables the construction of eminent PET-based biosensors. In this work I develop two classes of electron D-A dyads with high electron transfer efficiency; one is applied to photothermal energy conversion, and the other to singlet oxygen sensing applications. This thesis consists of five chapters, including the introduction to photoinduced electron transfer (chapter 1), where I summarise PET occurring in natural photosynthesis and its efficient mimicking toward the construction of various artificial solar energy harvesting systems. In the introduction chapter, I explain the classical theories of electron transfer in the designing of simple D-A dyads with efficient intramolecular electron transfer. In chapter 2, I discuss the synthesis of novel D-A systems, methods of characterization of D-A systems, and spectroscopic methods employed in the investigation of electron transfer and photothermal and sensing studies.

In chapter 3, I demonstrate the upgraded photothermal energy conversion by acridinium-based D-A dyads. Even though the conventional photothermal agents offer high energy conversion efficiency, most of them have narrow absorption bands. Therefore, broad band solar energy absorbing molecules and materials are continuously sought after. The general approach for the extension of light absorption by molecules to the entire UV-Visible-Near Infrared (UV-Vis-NIR) region is to extend the π-conjugation, which is tedious and time consuming. Thus, in this chapter, I employ a novel acridinium-based D-A dyad with highly-efficient electron transfer. Here I study the pH-dependent photothermal effect of a 9-position substituted acridinium-based D-A dyad with a phenolic OH group (**Acr1**).

The UV to blue absorbing dyad, **Acr1** undergoes efficient PET and subsequent deprotonation to form the betaine structure (**Acr1-betaine)** which absorbs the light in the UV-Vis-NIR region (Scheme 1). The generation of betaine intermediate is verified by the transient

absorption studies. **Acr1** shows substantial thermal response under blue light excitation and additional excitation of photoexcited **Acr1** with yellow light enables enhanced photothermal effect (PTE) which helps to utilize a broad spectrum of wavelength (Figure 1). The enhancement in PTE is discussed in terms of photoinduced betaine generation. The photothermal conversion efficiency of **Acr1** is 43 % with blue laser illumination, and the dual photoirradiation lifts the PTE. This study provides useful information to design and synthesize the variety of molecules to achieve upgraded light-harvesting properties from the additional excitation of the photogenerated species.

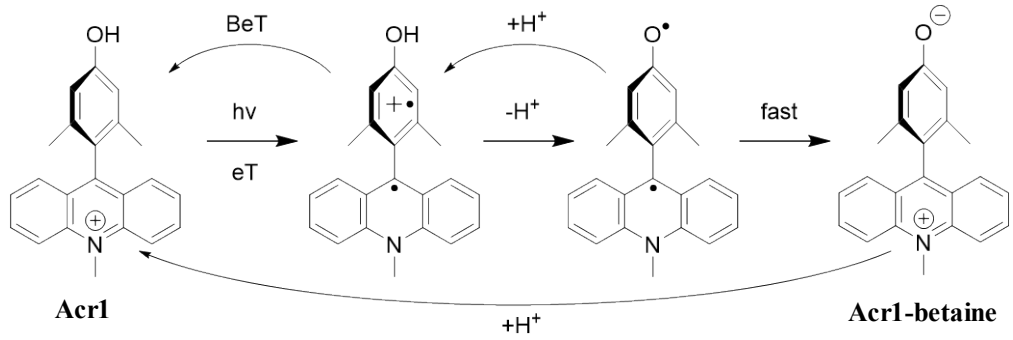

Scheme 1. The proposed scheme of PET and the subsequent deprotonation leading to the formation of **Acr1-betaine** from **Acr1**. eT: Electron transfer. BeT: Back electron transfer.

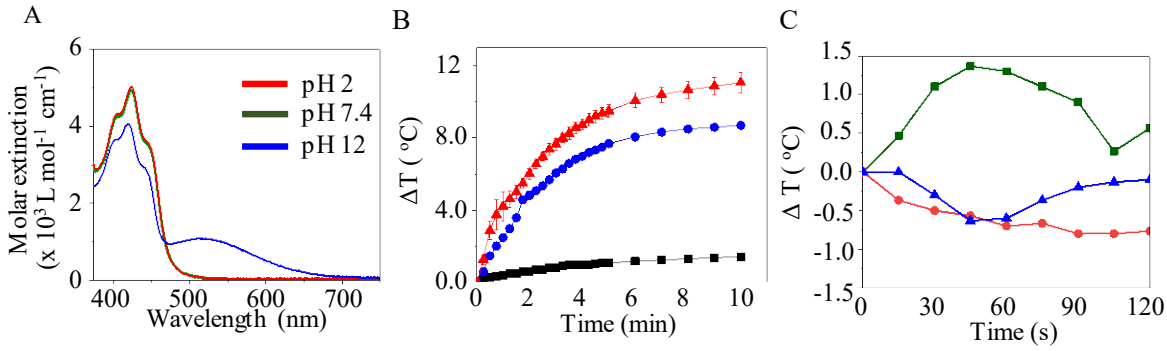

Figure 1. (A) pH dependent absorption spectra of **Acr1**. (B) The photothermal responses showed by **Acr1** at pH 7.4 due to the excitation with the blue light (420-440 nm, 140 mW cm^{-2}) (blue circle), a Xenon lamp (>480 nm, 440 mW cm^{-2}) (black quare), or the simultaneous excitation with both the light sources (red triangle). (C) The effective PTE which is enhanced by the dual photoexcitation of **Acr1** at pH 7.4 (green square), pH 2 (red circle) and pH 12 (blue triangle).

Singlet oxygen ($^1O_2$) gathers significant attention in chemistry and biology. There are several spectroscopic methods employ to detect $^1O_2$. Among these techniques, fluorescence sensing is one of the most promising method. Therefore, several anthracene-based electron D-

A dyads are reported. Although, the correlation between the structure of the sensor and the sensing efficiency needs further attention. In chapter 4, I study the kinetics of $^1O_2$ sensing by anthracene-based electron D-A dyads. I examine the $^1O_2$ sensing efficiency of three sensors, aminocoumarin-anthracene conjugates (**S1** and **S2**), and the Rhodamine 6G-anthracene conjugate (**S3**), and the model compound, 9-methylanthracene.

The fundamental structure of electron D-A based sensor is composed of an oxygen trapping moiety, which is anthracene, and a fluorescence reporter moiety. The sensing probe is in a fluorescence "off" state in the absence of $^1O_2$, which is by a dominant photoinduced intramolecular electron transfer from anthracene to the fluorescence reporter. The mechanism of sensing involves [4+2] cycloaddition reaction of $^1O_2$ to anthracene, leading to the formation of a 9,10-endoperoxide. Due to the endoperoxide formation, the PET is blocked to uncage the fluorescence and leading to the detection of $^1O_2$ (Scheme 2).

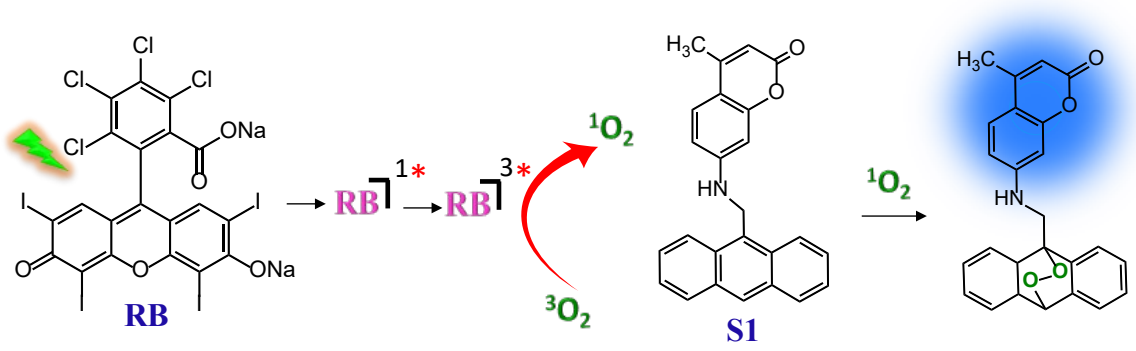

Scheme 2. A schematic representation of the Rose Bengal (RB) sensitized generation of $^1O_2$, and photooxidation of **S1** by $^1O_2$.

The $^1O_2$ sensing by the sensors is studied using fluorescence and absorption spectroscopic techniques (Figure 2). I determine the rates of the [4+2] cycloaddition reaction between $^1O_2$ and the molecular sensors using a second order rate equation (eq.1).

$$\ln\frac{C}{C_0} = -k\,\frac{\{C_0 - C - (\Delta C_{singlet\ oxygen}\ t)\}}{k_d} \qquad (1)$$

The second order rate of the oxidation of three sensors found to be an order of magnitude less than the model compound 9-methylanthracene. I hypothesize that the reduced reactivity is due to the steric effect of the bulky substituents or the truncated reactivity of the intermediate complex.

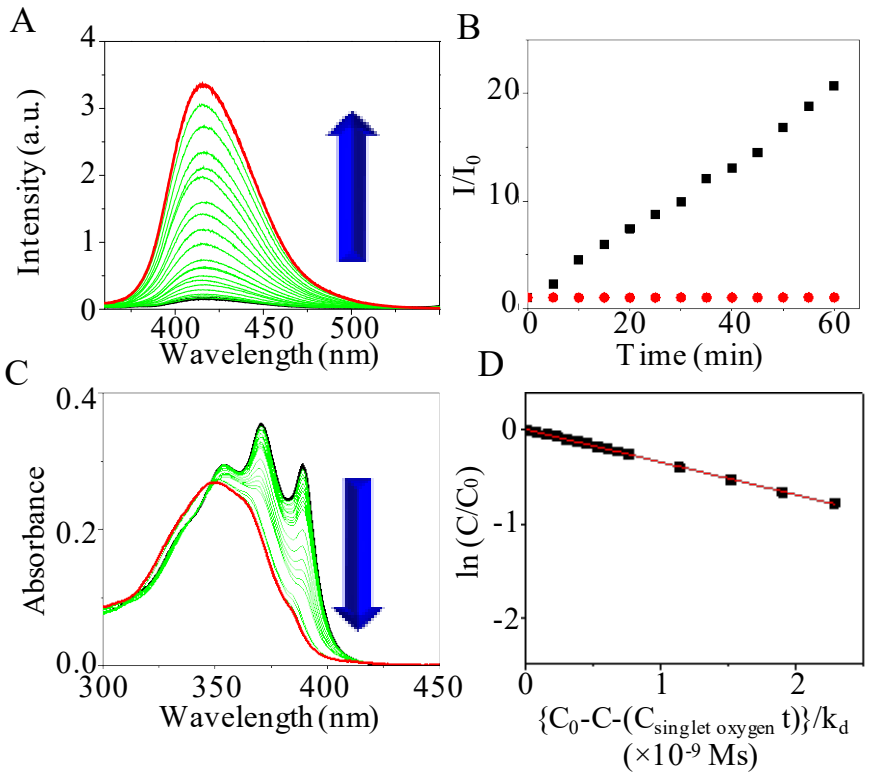

Figure 2. (A) Fluorescence (λ_{ex} 340 nm) and (C) absorption spectra of a solution of **S1** (10 μM) and RB (5μM) in DMF, before and after every 5 min intervals of photoactivation at 532 nm (50 $mWcm^{-2}$). (B) Time-traced relative fluorescence intensities, and (D) The second order kinetic plot of photooxidation of **S1** by $^1O_2$ constructed according to equation 1.

In chapter 5, I extensively study the mechanism of $^1O_2$ sensing by **S1** and rationalize the reduced sensing efficiency of **S1**. I found that UV illumination subsequent to the photosensitization of a sample solution of **S1** and RB show enormous fluorescence enhancement within 30 s (Figure 3). I hypothesize the existence of a less reactive intermediate complex which undergoes activated reaction under UV illumination. The intermediate persists for several hours and show significant stability towards $^1O_2$ scavengers. I confirm the role of coumarin substituent on the UV-activated reaction by using a Rhodamine 6G-based sensor (**S3**). To verify the existence of the intermediate complex between **S1** and $^1O_2$, I employ electron paramagnetic resonance spectroscopy (EPR) and nuclear magnetic resonance spectroscopy (NMR).

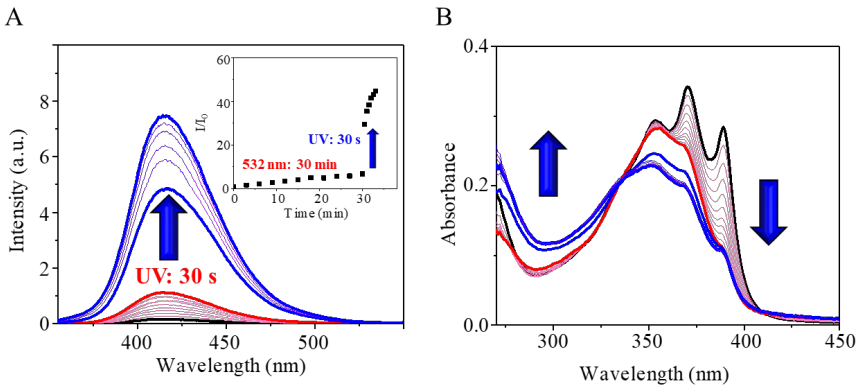

Figure 3. (A) Fluorescence spectra of a DMF solution of **S1** (10 μM) and RB (2:1 molar ratio) before and after every 5 min of photosensitization (λ=532 nm, 50 mW cm^{-2}), and photoactivation with UV (365 nm, 1 mW cm^{-2}) after 30 min of photosensitization. Inset: Time-traced relative fluorescence intensities of solutions of a mixture of **S1** and RB irradiated with 532 nm laser followed by illumination with UV lamp. (B) Absorption spectra of a DMF solution of **S1** (10 μM) and RB (2:1 molar ratio) before and after every 5 min of photosensitization (λ=532 nm, 50 mW cm^{-2}) for 30 min followed by photoactivation with UV (365 nm, 1 mW cm^{-2}).

I assume that $^1O_2$ reacts with **S1** to form a mixture of endoperoxide and an intermediate complex between $^1O_2$ and **S1**. By UV light illumination, the complex undergoes activated reaction to produce the endoperoxide at a higher rate, which is responsible for the enormous enhancement of the fluorescence (Scheme 3). Thus, the UV-activated reaction helps to improve the efficiency and speed of $^1O_2$ sensing.

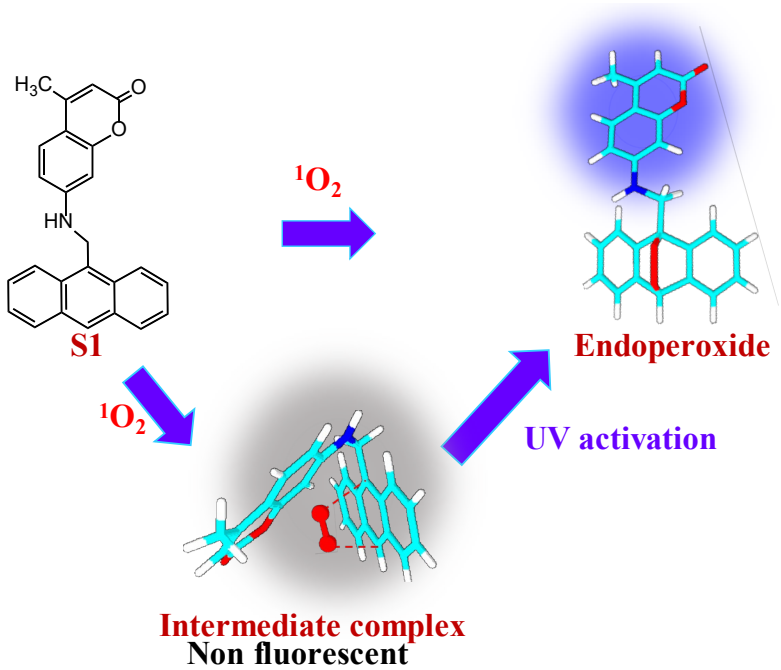

Scheme 3. Schematic representation of UV activated reaction of **S1** leading to enhanced fluorescence and enhancement in $^1O_2$ sensing efficiency.